A mechanistic study of hydrogen spillover in MoO_3 and carbon-based graphitic materials

2008 J. Phys.: Condens. Matter 20 064223

(http://iopscience.iop.org/0953-8984/20/6/064223)

J. Phys.: Condens. Matter **20** (2008) 064223 (7pp) doi:10.1088/0953-8984/20/6/064223

A mechanistic study of hydrogen spillover in MoO_3 and carbon-based graphitic materials

Liang Chen[1], Guido Pez[2], Alan C Cooper[2] and Hansong Cheng[2,3]

[1] Ningbo Institute of Materials Technology and Engineering, Chinese Academy of Sciences, Ningbo, Zhejiang 315201, People's Republic of China
[2] Air Products and Chemicals, Incorporated, 7201 Hamilton Boulevard, Allentown, PA 18195, USA

E-mail: chengh@airproducts.com

Received 1 August 2007, in final form 28 November 2007
Published 24 January 2008
Online at stacks.iop.org/JPhysCM/20/064223

Abstract

We present a systematic study of the mechanisms of the hydrogen spillover process from a Pt_6 cluster onto a well-known hydrogen bronze material, MoO_3, and several carbon-based materials, including a graphene sheet and single walled carbon nanotubes, using density functional theory (DFT). We show that initially hydrogen undergoes a sequential dissociative chemisorption upon interacting with the Pt_6 cluster. The threshold desorption energy of H atoms was identified. We then mapped out the energetics required for hydrogen atoms to flow onto the surfaces of the selected materials in the vicinity of the subnanometer Pt_6 particle and to diffuse to other sites of the substrates. Our results indicate that while the spillover of H atoms onto the MoO_3 lattice can be greatly facilitated by the abundant H-bonding network, the process becomes energetically difficult on carbon-based materials via chemisorption since it requires C–H bond breaking. Spillover in the selected carbon-based materials could only become possible if 'cold' H atoms could come out of the saturated catalyst.

(Some figures in this article are in colour only in the electronic version)

1. Introduction

As one of the key technologies required for the development of a hydrogen economy, hydrogen storage has recently become a subject of intensive research in materials science [1–5]. A wide variety of novel materials, ranging from light metal and chemical hydrides [2, 6, 7] to many carbon-based complexes [3–5], have been proposed in the last few years as potential storage media. Recently, Yang and co-workers developed a novel technique to store hydrogen via a 'hydrogen spillover' process [8, 9]. The method has generated considerable interest since an unusually high hydrogen storage capacity at ambient conditions can be achieved. It was hypothesized that in the 'spillover' process a flux of atomic hydrogen, generated via dissociative chemisorption of molecular hydrogen upon interaction with catalysts (i.e. platinum), first flows from catalytic particles to the substrate via an adsorption process through a 'bridge' built with carbonized sugar and subsequently diffuses throughout the materials [8, 9]. Apparently, to achieve the high storage capacity, it is essential that the adsorbed hydrogen atoms should be nearly free to move to other adsorption sites far from where the catalysts reside. To adequately address the spillover mechanism on support materials, it is critical to understand the entire spillover process including the chemical and transport behavior of the H atoms adsorbed. Unfortunately, to date, the detailed mechanisms of hydrogen spillover on support materials are still poorly understood since the published studies have only addressed a few selected steps of the spillover processes.

In this paper we attempt to address theoretically the entire hydrogen spillover processes in several materials on which spillover is known and/or reported to occur. The thermochemical energies and energy barriers required for hydrogen atoms to flow onto the substrate surfaces located in the vicinity of subnanometer platinum catalyst particles and

[3] Author to whom any correspondence should be addressed.

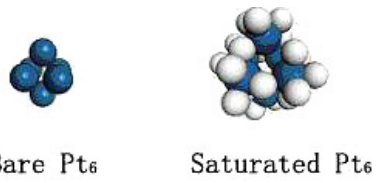

Figure 1. The optimized geometries of the bare Pt_6 cluster and Pt_6/H_n.

subsequently to diffuse to other sites of the materials were calculated. The systems selected in the present study include MoO_3, a graphene sheet and two armchair carbon nanotubes. MoO_3 is a material in which hydrogen spillover is known to readily occur [10–13]. Despite the fact that this material has been widely used experimentally as a hydrogen reservoir for catalytic hydrogenation [10–13], the underlying spillover mechanisms have not been well understood. Studies on the detailed hydrogen spillover processes in MoO_3 could shed light on spillover in carbon-based materials. Some of the carbon-based materials selected in the present study have been used by Yang and co-workers to demonstrate the spillover process [8, 9]. We expect that detailed comparative studies between the well-known spillover systems, such as MoO_3, and the selected carbon-based materials would help enhance our understanding of spillover mechanisms in materials of interest for hydrogen storage.

2. Theoretical models and computational methods

To simplify the description of spillover on the support materials we chose a small octahedral platinum cluster, Pt_6 (as shown in figure 1), to represent the catalyst particle. The cluster is obviously too small compared to the size of catalyst particles used in experiments. However, when used in the study of catalyst–substrate interface it can still yield useful physical insights into the catalytic reaction processes. Furthermore, a recent DFT study by Zhou *et al* indicates that some of the important properties, such as H_2 dissociative chemisorption and H desorption energies at full cluster saturation, do not change significantly with cluster size [14]. The calculations were performed using density functional theory under the generalized gradient approximation with the Perdew–Wang exchange–correlation functional (PW91) [15]. The spin-polarization scheme was employed throughout to deal with the electronically open-shell systems. For the sequential dissociative chemisorption of H_2 on an isolated Pt_6 cluster, the calculations were first performed using the DMol^3 package [16]. A double numerical basis set augmented with polarization functions was utilized to describe the valence electrons, with the core electrons described with an effective core potential, which also accounts for the relativistic effect that is important for heavy elements such as platinum. To avoid computational bias, the cluster and H_2 chemisorption geometries were fully optimized without imposing symmetry constraints until the energy is converged to less than 2×10^{-4} eV, the maximum force is less than 0.05 eV Å^{-1} and the maximum displacement is less than 0.005 Å.

The MoO_3 solid has a layered structure. Each layer is a natural slab of the MoO_3 (010) surface comprising two symmetric Mo–O sheets (upper and lower) linked by strong Mo–O bonds. There are three structurally distinct lattice oxygen atoms on each sheet, i.e. terminal oxygen, symmetric bridging oxygen and asymmetric bridging oxygen as shown in figure 2. Two binding modes are identified on the upper asymmetric oxygen: bound perpendicularly to the surface, noted as $A_{\mathrm{upp},p}$, or bound at an angle directly pointing toward the lower asymmetric oxygen, noted as $A_{\mathrm{upp},i}$. The binding mode A_{low} on the lower asymmetric oxygen is equivalent to $A_{\mathrm{upp},i}$ considering the symmetry of the MoO_3 slab. On the symmetric oxygen, one binding mode, noted as S_{upp}, is identified. In this study, a supercell containing one $(2 \times 2)MoO_3$ (010) layer and an 18 Å vacuum space was selected.

A symmetric slab supercell containing one (5×5) graphene sheet and a 16 Å vacuum space was used to model the graphite (0001) surface. The supercell contains 50 carbon atoms, with a dimension of 12.2 Å × 12.2 Å × 16 Å. The spillover of H on the SWNTs was simulated in a rectangular supercell containing one isolated SWNT with two primitive unit cells. The size of the supercell is 20 Å×20 Å×7.4 Å. Only the case in which there is only one C–H bond in the selected supercell was studied. It is anticipated that both the calculated reaction energies and activation barriers will be higher if more C–H bonds are involved since a higher number of C–H bonds with energetically favorable conformation would prevent the C–H bond from dissociation and thus give rise to a higher activation barrier. We thus expect that the cases selected for study would give a lower bound of the energy required for an H atom to diffuse to other C atoms.

All calculations on materials involved in hydrogen spillover at the catalyst–substrate interface and subsequent H surface diffusion were performed using the Vienna *Ab Initio* Simulation Package (VASP) [17, 18]. The electron–ion interactions were described by the projector augmented wave (PAW) pseudopotentials [19, 20]. An energy cutoff of 400 eV was used to make sure that the total energy is well converged. All atoms were fully relaxed with the forces converged to less than 0.05 eV Å^{-1}. The nudged elastic band (NEB) method [21, 22] was used to determine the minimum energy pathways for H diffusion.

3. Results and discussion

3.1. Hydrogen chemisorption on Pt_6

The optimized bare Pt_6 structure is shown in figure 1. The calculated nearest neighboring Pt–Pt bond length in the cluster is 2.72 Å, which is about 0.06 Å shorter than in the bulk. Three possible adsorption sites for dissociated H_2 on the chosen Pt_6 cluster are identified: one-fold on top, two-fold bridge and three-fold hollow site. Calculations of dissociative chemisorption of a H_2 molecule at these sites yielded chemisorption energies of 1.71 eV, 1.50 eV and 1.31 eV, respectively, indicating that the on-top adsorption configuration is energetically most favorable. A recent desorption experiment of H/D from a Pt_{12} cluster yielded an

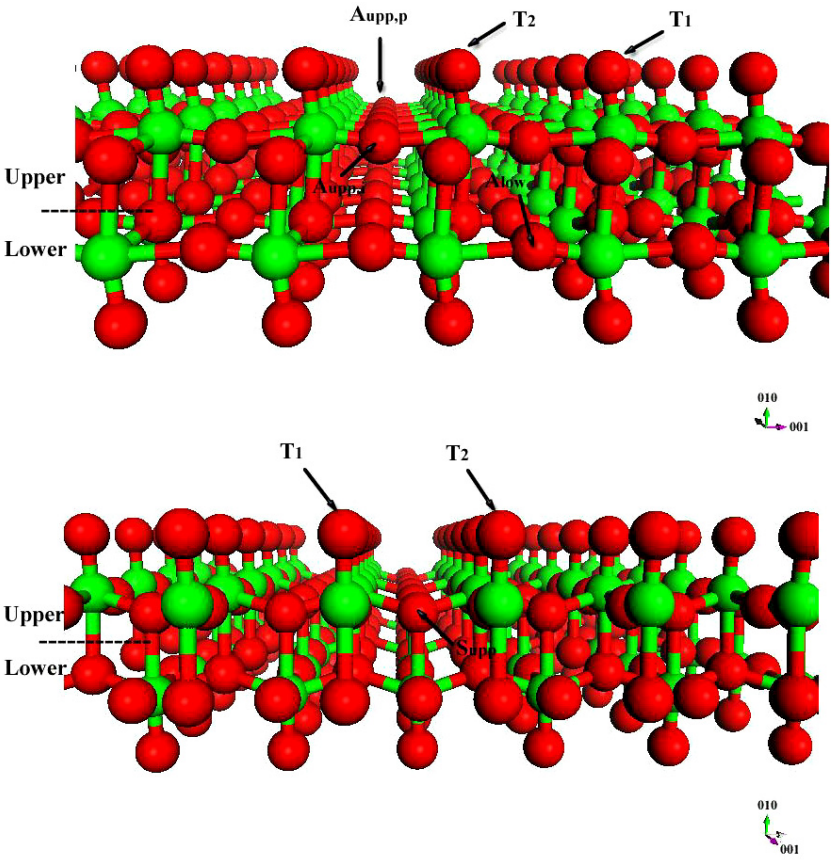

Figure 2. The one-layer model of the MoO_3 (010) surface. The red (darker) spheres are oxygen atoms, the green (lighter) spheres are Mo atoms. The arrows represent the orientation of the H–O bond.

H_2 dissociation chemisorption energy of 1.36 eV [23], which is slightly lower than our calculated values. However, this is not surprising since smaller clusters usually possess higher reactivity toward H_2 dissociation chemisorption.

Under a realistic catalytic condition an adequate H_2 pressure is usually maintained and thus the catalytic particles are always fully saturated by hydrogen atoms. Hence, we next allowed H_2 molecules to undergo further dissociative chemisorption on the Pt_6H_2 cluster. The H atoms first populate at the on-top sites with each Pt atom adsorbing two H atoms since chemisorption at these sites is energetically most stable. Upon saturation of all the on-top sites at $n = 12$, the bridge sites, at which chemisorption of H is less stable than at the on-top sites but more stable than at the three-fold face sites, could also be populated until $n = 24$. However, no H adsorption at the three-fold face sites was found. At $n = 24$, the Pt_6 cluster appears to reach the full saturation with atomic H. The Pt/H ratio at $n = 24$ is 1:4. Indeed, attaching two more H atoms to the Pt_6H_{24} cluster yielded a H_2 molecule weakly bonded to the cluster upon running an *ab initio* molecular dynamics simulation at 300 K using a Nosé–Hoover chain thermostat [24] for 2 ps, suggesting that no more H atoms can be accommodated on the cluster. The fully optimized chemisorption structure of Pt_6H_{24} is displayed in figure 1. It is noteworthy that considerable structural distortion of the Pt_6 cluster from the original symmetric octahedral geometry was observed upon dissociative chemisorption of H_2. At a low H coverage, the bond lengths of H-bonded Pt–Pt are elongated by 0.05–0.2 Å, while the bond lengths of non-H-bonded Pt–Pt are shortened by 0.05–0.1 Å. At a high H coverage, all Pt–Pt bond lengths are elongated by 0.01–0.3 Å since all Pt atoms are directly bonded with hydrogen atoms.

A central issue in heterogeneous catalysis is how to determine the minimum energy required for the H atoms to come off the metal catalyst as atomic hydrogen under a typical catalytic condition. We propose that this minimum energy, or more precisely the threshold H desorption energy, is not the average desorption energy of H atoms. Instead, it should be the sequential H desorption energy, defined as

$$E_{\mathrm{sd}} = E(\mathrm{H}) - [E(\mathrm{Pt_6H}_n) - E(\mathrm{Pt_6H}_{n-2})]/2, \qquad (1)$$

at the full cluster saturation, where $E(\mathrm{H})$ is the energy of the H atom and $n = 2, 4, 6, \ldots$. This is because desorption of an H atom from the cluster would make a space available to accommodate another atom resulting from H_2 dissociative chemisorption and the metal clusters should always be in the fully saturated state under typical catalytic conditions. As shown in figure 3, the calculated sequential H desorption energy decreases monotonically with the H coverage on the cluster, indicating that as the H loading on the cluster increases it becomes easier for H atoms to desorb from the cluster to participate in a catalytic reaction. At the full saturation, the

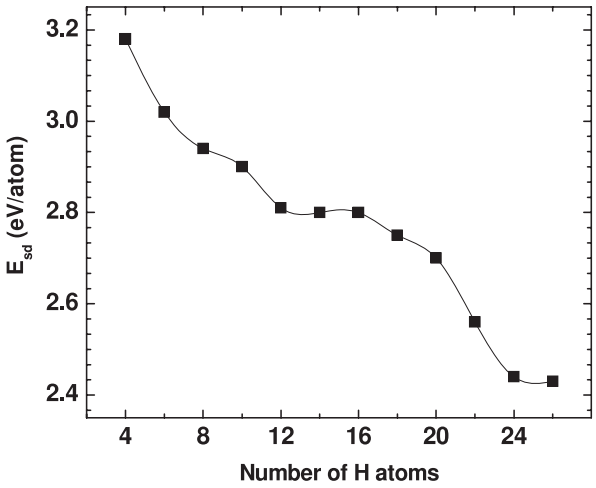

Figure 3. The calculated sequential H desorption energy on a Pt_6 cluster.

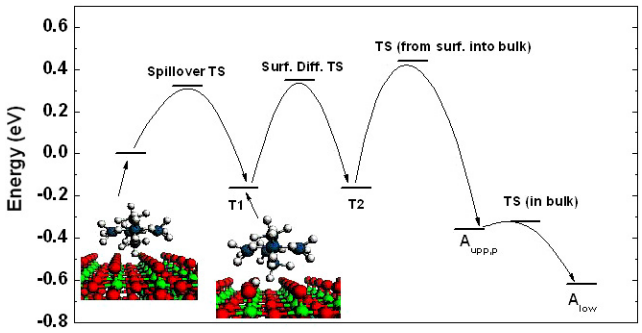

Figure 4. Energetic profile of hydrogen spillover from Pt_6 to the MoO_3 (010) surface and subsequent migration from the surface into bulk.

calculated threshold H desorption energy is 2.44 eV, which is significantly lower than the average H desorption energy of 2.81 eV and the H desorption energy of 3.2 eV at zero coverage.

3.2. H spillover from Pt_6 onto MoO_3

Upon obtaining the structure of the fully saturated H_{24}/Pt_6 cluster, we can study hydrogen spillover from the Pt_6 catalyst onto the MoO_3 (010) surface. The pre-optimized saturated H_{24}/Pt_6 cluster was initially placed 2.5 Å above the MoO_3 slab and then gradually brought down to the surface to simulate the interface reaction. Full geometric optimization, except for the designated reaction coordinate along the surface normal, was performed until all forces were converged to less than 0.03 eV $Å^{-1}$. The calculated energy profile along the diffusion pathway shows that an H atom can desorb readily from the H_{24}/Pt_6 cluster and diffuses onto the terminal oxygen to form an O–H bond with a low energy barrier of 0.32 eV. Compared to the aforementioned 2.44 eV threshold energy, the H desorption energy from the Pt_6 cluster is significantly reduced upon the cluster interaction with the substrate as shown in figure 4. The migration process is exothermic with a reaction energy of 0.15 eV. The calculated low activation barrier of 0.3 eV is consistent with the experimental observation that hydrogen spillover can readily occur in this system [10–13]. The Bader charge analysis [25] revealed that this low barrier is a result of charge flow and protonation. Upon H migration from the Pt_6 cluster onto the terminal oxygen, the electrons begin to flow from the H-1s orbital to the O-2p orbital. The migrated H atom loses its electron and turns out to be positively charged by +0.96. It is also noteworthy that the remaining hydrogen atoms adsorbed on Pt_6 all partially lose their electron with charges on the atoms ranging from +0.05 to +0.15 electrons. As a result, the oxygen atoms gain extra electrons and thus loosen the Mo–O bond.

Figure 4 also shows the calculated activation barriers of hydrogen migration from the vicinity of Pt_6 into the MoO_3 bulk following a selected pathway. The second barrier with a height of 0.51 eV between states T1 and T2 (as shown in figure 2) corresponds to the hopping between two adjacent terminal oxygen atoms. This relatively low activation barrier again suggests that the H migration on the surface can be facile at moderate temperatures. The next barrier between T2 and $A_{\mathrm{upp},p}$ corresponds to diffusion from the terminal oxygen onto the upper asymmetric oxygen as shown in figure 2. The calculated activation energy is 0.6 eV. This slightly higher energy indicates that the diffusion from the surface (terminal) oxygen into the bulk might be the rate-limiting step for the hydrogen spillover. Two binding modes have been identified on the asymmetric oxygen: $A_{\mathrm{upp},p}$ and $A_{\mathrm{upp},i}$. Our calculation on the H migration in the lattice reveals that the H atom is able to rotate around the ⟨001⟩ direction by 120° from $A_{\mathrm{upp},p}$ to $A_{\mathrm{upp},i}$ with nearly zero activation energy. Hence, in the entire proton spillover pathway the highest activation barrier is no more than 0.6 eV, which clearly explains the high mobility of H in the whole process. A careful analysis of the lattice structure of MoO_3 indicates that the distance between any two adjacent O atoms is around or less than 3.0 Å. Hence, hydrogen can always maintain H-bonding with at least one O atom during the migration owing to their 'crowded' oxygen neighbors. This special structure can enable an effective H-bonding network for hydrogen migration and thus significantly reduce the migration barrier energy.

3.3. H spillover from Pt_6 to a graphene sheet

We next studied H spillover from the saturated Pt_6 cluster onto a graphene sheet using a similar computational scheme as for the H_xMoO_3 calculation. The 'bridge' utilized in the experimental study by Yang *et al* was not incorporated in the theoretical model since its exact composition and structure are unknown. The calculated energy profile for H spillover from the Pt_6 cluster to the graphene sheet is shown in figure 5. The process resulting in migration of two H atoms from the catalyst to the graphene sheet to form two C–H bonds is slightly endothermic thermodynamically with an average reaction energy of 0.23 eV per H atom. In contrast to the high H desorption energy in the fully saturated Pt_6 cluster, the calculated average activation barrier for the migration is 0.48 eV per H atom, indicating that the process might be kinetically facile as well. Hence, H migration from Pt catalyst

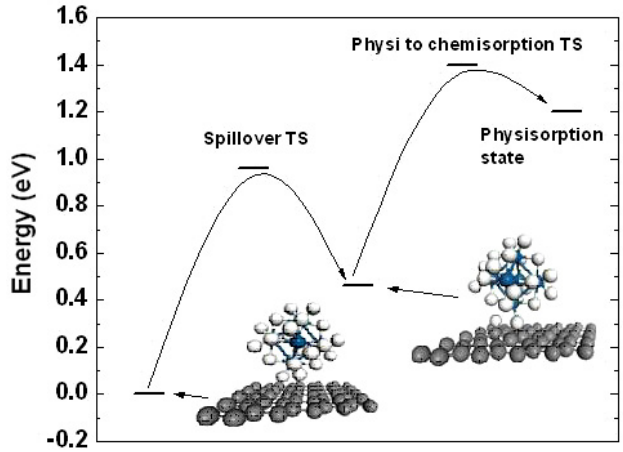

Figure 5. Energetic profile of hydrogen spillover from Pt_6 onto a graphene sheet and diffusion between physisorption and chemisorption states.

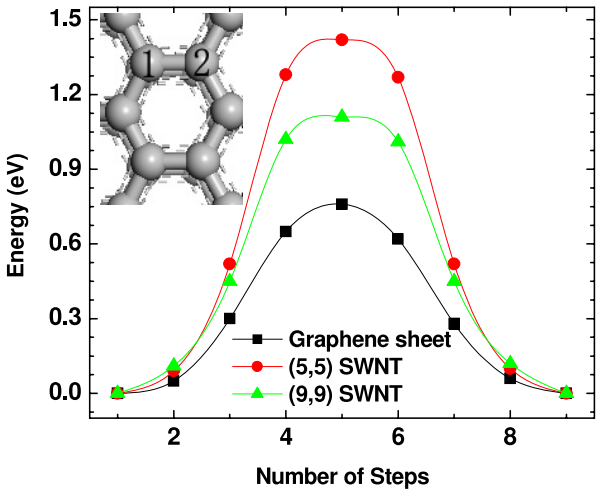

Figure 6. H diffusion between adjacent sites in the chemisorption region on a graphene sheet and two SWNTs; the line is drawn as a guide to the eyes.

to graphene sheet at the vicinity of the catalyst can occur at ambient conditions. In the experiments conducted by Yang and co-workers, the Pt catalyst nanoparticles are dispersed on a support glued together with a bridge material made of carbonized sugar. These materials may prevent the catalyst particles from direct contact with the substrate. We speculate that H atoms can still come out of the catalyst and pass through the surfaces of the support to enter the substrate surfaces [26]. Depending on how energetic these H atoms are, they may stay on the surfaces via a chemisorption or a physisorption process. Figure 5 also displays the calculated potential energy profile for an H atom to approach to a graphene sheet from the surface normal. It first enters the physisorption state at a large distance. Starting at a distance of approximately 2.5 Å, the potential energy becomes slightly repulsive until at around 2.2 Å, after which the energy decreases rapidly and a C–H bond is then formed. The calculated energy barrier is about 0.2 eV, which agrees with the value reported by Sha and Jackson [27]. Detailed structural examination indicates that the underneath C atom must come out of the graphene plane in order to form a C–H bond with the incoming H atom, which imposes strain on the neighboring C atoms and thus gives rise to the barrier. Therefore, if the H atoms coming out of the catalyst become sufficiently 'cold' after moving through the surfaces of support and/or 'bridge', it is possible that they could be blocked by the barrier and thus become physisorbed on the substrate surface. The calculated physisorption energy on the graphite and SWNTs for the H atom is less than 0.1 eV. On the other hand, if the H atoms are 'hot', they can easily overcome the barrier to form strong covalent C–H bonds with the graphitic C atoms.

3.4. H diffusion on carbon-based materials

A key issue concerning the mechanism of hydrogen spillover, therefore, is whether the H atoms, regardless of physisorption or chemisorption, are able to diffuse throughout the substrates. We first examined the situation of chemisorption, which leads to C–H bond formation, in several carbon-based materials including a graphene sheet and two armchair single walled carbon nanotubes (SWNTs), (5, 5) and (9, 9).

Figure 6 displays the calculated potential energy curves for an H atom to move from a C atom to an adjacent C atom (site 1 to site 2, as shown in the inset) on a graphene sheet and two SWNTs. The calculations yield activation energies of 0.78 eV on the graphene sheet, which is close to the adsorption energy of an H atom on the substrate but slightly lower than the activation energy required to desorb from the surface. This result indicates that the C–H bond needs to be broken in order for the H atom to move to an adjacent C atom to form another C–H bond. Apparently, this stringent requirement hinders H diffusion. Upon H diffusion, the puckered carbon atom moves back toward its original lattice site. Simultaneously, the adjacent carbon atom is pulled out to form a new C–H bond. For H diffusion from site 1 to its second nearest neighbor, the calculated minimum energy pathway indicates that the H atom must pass through site 2. Therefore, the calculated potential energy curve for the diffusion pathway is simply a duplicate of figure 6.

The calculated H diffusion activation energies for an H atom to move to an adjacent C atom are 1.42 and 1.09 eV on the (5, 5) and (9, 9) SWNTs, respectively. Similarly, these values are very close to the corresponding adsorption energies, again indicating C–H bond breaking upon diffusion. The calculated energy profiles reflect the strong influence of the SWNT curvature. A large curvature positively enhances the adsorption strength, but also significantly reduces the mobility of H on the surface and thus the effectiveness of the spillover process. Compared with the results on the graphene sheet, it is more difficult for the H atom to diffuse on the sp^3-like carbon atoms.

Figure 7 displays the calculated potential energies along the H diffusion pathway from site 1 to 3 as shown in the inset for a graphene sheet and two SWNTs. It exhibits a double hump feature representing essentially three consecutive

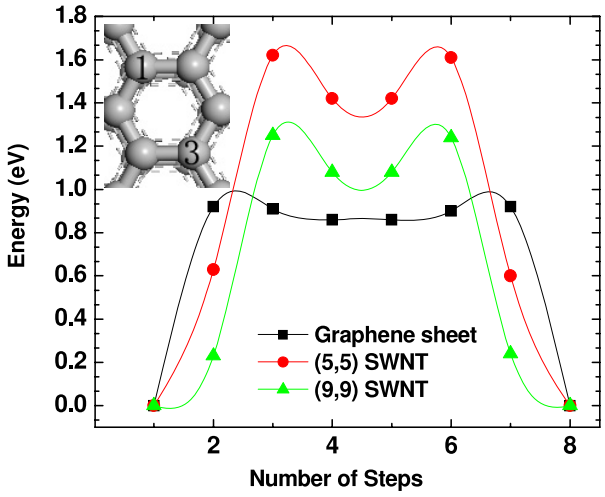

Figure 7. H diffusion from site 1 to 3 in the chemisorption region on a graphene sheet and two SWNTs; the line is drawn as a guide to the eyes.

steps for all three materials. First, an H atom is desorbed from the surface. Subsequently, the atom is adsorbed at a metastable site above the center of the hexagonal ring. Finally, it moves to its destination by forming a covalent C–H bond at site 3. For a graphene sheet, the rate-limiting step is the transition from the chemisorption state to the metastable site with a barrier of 0.95 eV, which is slightly higher than the activation energy of diffusion between two adjacent sites. Considering the small difference of 0.17 eV, it is likely that the two diffusion pathways may coexist at an elevated temperature. The calculated activation energies for H diffusion from site 1 to 3 are 1.61 and 1.29 eV on the (5, 5) and (9, 9) SWNTs, respectively. These results show that the H atoms are unlikely to diffuse freely at ambient temperatures and pressures. The curvature effect on the diffusion becomes more pronounced as the radii of the materials get smaller.

Our results suggest that H mobility on the selected carbon materials is considerably hindered by the formation of C–H bonds upon chemisorption and H diffusion becomes increasingly difficult with the increase in carbon curvature. Hydrogen spillover is thus difficult if C–H bonds are formed. We speculate that the spillover phenomena observed in experiments were dictated by an H physisorption process. Physisorption of hydrogen atoms on graphitic materials has already been observed in an experiment [28]. Our calculations concerning the movement of physisorbed H atoms in the physisorption region, i.e. at least 2.5 Å above the surface, yield very little change in potential energy, suggesting that H diffusion in the physisorption region is facile.

Indeed, in a recent report, Ye and Chiu claimed that atomic hydrogen is mobile on graphite at room temperature, based on their observations in an experiment on graphite-mediated reduction of azoaromatic compounds with elementary iron in dialysis cells [28]. We suspect that hydrogen spillover in carbon-based materials is mainly driven by some kinetically 'cold' H atoms that reside in the physisorption region.

4. Summary

Hydrogen spillover onto carbon-based materials represents a novel technique for storing hydrogen in a variety of materials that are readily available. In order to systematically study the underlying mechanisms that govern the spillover process in carbon-based materials, we performed extensive first-principles based calculations on hydrogen interaction with materials in which spillover phenomena were known or reported to take place. The spillover process was broken into three consecutive steps and we have carefully investigated each step by extensively searching for the minimum energy pathways to obtain H adsorption/diffusion structures and energetics. The first step involves the sequential H_2 dissociative chemisorption on a Pt_6 cluster until the cluster is fully saturated. The threshold H desorption energy from the cluster was then obtained. In the second step, the Pt catalyst fully saturated by H atoms delivers H atoms to the substrate surfaces. In the third step of the hydrogen spillover process, we studied diffusion of an H atom chemisorbed on surfaces and in bulk of the substrate materials.

The migration of H atoms from the catalyst to the substrate may involve chemisorption and/or physisorption processes. Our computational results indicate that the chemisorption process might be able to proceed readily at ambient conditions with small to moderate activation barriers and nearly thermoneutral reaction energies.

For hydrogen in MoO_3, which is a well-known spillover system, our results suggest that H migration from the Pt_6 cluster to the substrate is facilitated by forming H-bonds with the terminal O atoms and thus the process is facile at ambient conditions. The migration gives rise to protonation to form hydrogen bronze. The H atoms can further diffuse into the entire lattice of the material with favorable thermodynamics and relatively low activation barriers. The diffusion was made facile by the abundant H-bonding network in the lattice.

For H migration to the selected carbon-based materials via a chemisorption process to form C–H bonds, both the calculated H-bond strengths and diffusion barriers were found to be curvature dependent with the higher adsorption energy and the diffusion barriers associated with the carbon atoms of larger curvatures. Our results suggest that it would be difficult for the H atom to move freely on a graphene sheet and SWNTs at a moderate temperature since its diffusion would lead to C–H bond breaking, which requires substantial activation energy. On the other hand, H atoms may also undergo a physisorption process to stay on the surfaces of the carbon materials. With the minimum H desorption energy of approximately 2.4 eV from the fully saturated Pt cluster, we speculate that this process could only be induced by the support and/or bridge materials. If these H atoms are 'hot' upon migration, they will immediately form a bond with a carbon atom nearby. If they are sufficiently 'cold', the H atoms will be physisorbed at least 2.5 Å above the graphitic surfaces, in which H diffusion throughout the surfaces is energetically feasible. An interesting question is how stable the physisorbed H atoms are on the surfaces of carbon materials. Our preliminary results on collisions of physisorbed H atoms with C_{60} at room

temperature using *ab initio* molecular dynamics suggest that these H atoms can readily recombine to form H_2 molecules or form C–H bonds with C_{60} if they gain enough momentum [29]. In other words, physisorbed H atoms would rarely stay in a stable state at a finite temperature. Finally, our computational results suggest that it is easier for hydrogen spillover to occur in MoO_3 than in the selected carbon-based materials. The underlying mechanisms in these two types of materials are also distinctively different.

Acknowledgments

This work is partially supported by the US Department of Energy via the Center of Excellence of Carbon-based Hydrogen Storage Materials.

References

[1] Schlapbach L and Zuttel A 2001 *Nature* **414** 353
[2] Rosi N L, Eckert J, Eddaoudi M, Vodak D T, Kim J, O'Keeffe M and Yaghi O M 2003 *Science* **300** 1127
[3] Chen P, Xiong Z T, Luo J Z, Lin J Y and Tan K L 2002 *Nature* **420** 302
[4] Liu C, Fan Y Y, Liu M, Cong H T, Cheng H M and Dresselhaus M S 1999 *Science* **286** 1127
[5] Dillon A C, Jones K M, Bekkedahl T A, Kiang C H, Bethune D S and Heben M J 1997 *Nature* **386** 377
[6] Løvvik O M and Opalka S M 2005 *Phys. Rev.* B **71** 054103
[7] Luo W and Gross K J 2004 *J. Alloys Compounds* **385** 224
[8] Li Y and Yang R T 2006 *J. Am. Chem. Soc.* **128** 8136
[9] Li Y and Yang R T 2006 *J. Phys. Chem.* B **110** 17175
[10] Hoang-Van C and Zegaoui O 1997 *Appl. Catal.* A **91** 164
[11] Hoang-Van C and Zegaoui O 1995 *Appl. Catal.* A **130** 89
[12] Sakagami H, Asano Y, Takahashi N and Matsuda T 2005 *Appl. Catal.* A **284** 12
[13] Šušic M V and Solonin Y M 1988 *J. Mater. Sci.* **23** 267
[14] Zhou C, Wu J, Nie A, Forrey R C, Tachibana A and Cheng H 2007 *J. Phys. Chem.* C **111** 12773
[15] Perdew J P, Chevary J A, Vosco S H, Jackson K A, Pederson M R, Singh D J and Fiolhais C 1992 *Phys. Rev.* B **46** 6671
[16] DMol^3 2005 Accelrys Software, Inc., San Diego
[17] Kresse G and Hafner J 1993 *Phys. Rev.* B **48** 13115
[18] Kresse G and Furthmuller J 1996 *Comput. Mater. Sci.* **6** 15
[19] Kresse G and Joubert J 1999 *Phys. Rev.* B **59** 1758
[20] Blochl P E 1994 *Phys. Rev.* B **50** 17953
[21] Mills G, Jónsson H and Schenter G K 1995 *Surf. Sci.* **324** 305
[22] Jónsson H, Mills G and Jacobsen K W 1998 Nudged elastic band method for finding minimum energy paths of transitions *Classical and Quantum Dynamics in Condensed Phase Simulations* (NJ: World Scientific)
[23] Liu X, Dilger H, Eichel R A, Kunstmann J and Roduner E 2006 *J. Phys. Chem.* B **110** 2013
[24] Martyna G J, Tuckerman M E and Tobias M E 1996 *Mol. Phys.* **87** 1117
[25] Bader R F W 1990 *Atoms in Molecules—A Quantum Theory* (New York: Oxford University Press)
[26] Lachawiec A J, Qi G and Yang R T 2005 *Langmuir* **21** 11418
[27] Sha X and Jackson B 2002 *Surf. Sci.* **496** 318
[28] Ye J and Chiu P 2006 *Environ. Sci. Technol.* **40** 3959
[29] Knippenburg M T and Cheng H 2008 in preparation